Experimental Investigation of Hydrodynamics on Abrupt-Expansion Pipe Behind Control Valve of Hydro-Driven Shiplift

Jiao Wang[1(⊠)] and Yaan Hu[2]

[1] Southwest Hydroengineering Research Institute for Waterway,
Chongqing Jiaotong University, Chongqing 400016, China
`1004612079@qq.com`
[2] Nanjing Hydraulic Research Institute, Nanjing 210029, Jiangsu, China

Abstract. Control valve is the special core equipment of hydro-driven ship lift, it is similar to the electric motor of the electric driven ship lift, which is the key to the safe and efficient operation of ship lift. Hydro-driven ship lift requires very high performance of control valve. It not only needs to control the flow accurately, but also to meet the needs of large flow. It is difficult to avoid cavitation for control valve to work under high pressure difference. How to control the erosion and destruction of valves and pipelines caused by cavitation is related to the operation safety and efficiency of hydro-driven ship lift. Sudden expansion of pipe behind the valve is a simple and efficient valve cavitation suppression technology. Aiming at typical control valve (plunger valve), this paper uses physical model tests and theoretical analysis to study the effect of sudden expansion of pipe behind the valve on the flow resistance characteristics of valves, and comprehensively consider the effects of valve type, flow pattern, and flow pulsation. According to the analysis, the relationship between sudden expansion ratio of the pipe and valve flow coefficient is obtained, and the test results are in good agreement with the theoretical analysis. Based on the theoretical analysis and considered the effect of cavitation defense, the expansion ratio for this type of abrupt expansion pipe is suggested to be 3.00. This study has guiding significance for the anti-cavitation technology of industrial valves, and can be used as a reference for the design of pipelines for water delivery and pressure regulation projects.

Keywords: Control valve · Cavitation · Flow coefficient · Sudden expansion ratio

1 Introduction

Hydraulic driven shiplift (HDSL) is a new attempt on high dam navigation technology in the world. It mainly uses water power as the lifting power and security measure. The ship reception chamber moves with the rise and fall of the buoys in the vertical shafts, which are driven by the filling and emptying system. When the ship chamber load is changed, the submerged depth of the buoys will have a corresponding change to make the ship chamber reach a new equilibrium between chamber and buoys, and solve the

serious leakage problem in ship chamber, which is an incomparable technical advantage than traditional electric driven shiplift (Hu 2011). It is especially suitable for high dam navigation, and has a broad application prospect. Jinghong shiplift is the first HDSL in the world (Fig. 1).

The filling and emptying system of HDSL is similar to the electric drive system of traditional shiplift, which is the source of power. Its running speed and acceleration are controlled through the precise regulation of water flow. Hence, the performance of the valve plays an important role in the safety and stability of HDSL.

Cavitation is a transition phase between liquid and cavitation bubbles which occur within low pressure zone and crush with pressure recovery (Pan et al. 2013). Cavitation is a very common hydraulic phenomenon in hydraulic machinery such as propellers (Pennings et al. 2016), venturi tubes (Bertoldi et al. 2015), vane pumps (Li 2016), and control valves (Hubballi et al. 2013). Studies of valve cavitation always focus on noise, vibration, and performance reduction (Shirazi et al. 2012). Most research still relies on experiments (Long et al. 2018) with a variety of measurement methods such as high-speed photography (Wang et al. 2015), PIV (Kravtsova et al. 2014), probes (Pham et al. 1999), and observation window (Osterman et al. 2009). With the fast development of CFD (computational fluid dynamics), numerical simulations have also been used to study cavitation inside the valves and other situations beyond the capability of experiments (Liu et al. 2006).

Cavitation should be controlled for the safety and efficiency of HDSL. Based on the mechanism of cavitation, the cavitation defense measures for control valves are mainly divided into two categories: aeration (Tomov et al. 2015) and structure optimization (Gholami et al. 2015). Chern studied the globe valve with or without a cage by cavitation model (Chern et al. 2004). The results indicated that the cage could limit the cavitation to the vicinity of cage and prevent cavitation to erode valve body and downstream pipe. Hubballi performed analytic and experimental research by using cavitation index to predict the cavitation effects for hydraulic control valves. Jo made a numerical study for reducing cavitation in butterfly valve (Jo et al. 2013), and the perforated plate was thought to be effective to suppress the cavitation inside of the pipe. Gholami studied the needle valve by 3-D numerical simulation. A circular row of vanes was used at the end section of the needle valve. From their study, they concluded that cavitation was suppressed, but the flow coefficient also was decreased. Lee made a shape design of bottom plug used in a 3-way reversing valve to minimize the cavitation effect (Lee et al. 2016). Han selected three kinds of typical structures of poppet valves to research (Han et al. 2017). The results revealed that two-stage throttle valve (TS valve) can effectively suppress the occurrence of cavitation while the flow force of TS valve was much bigger than other valves.

The present researches about industrial valve cavitation, mainly concentrate on the cavitation mechanism and the structure optimization of valve. In the conditions of high pressure and large flow rate, there have few researches about useful measures which can be applied to practical engineering for efficiently restraining cavitation. In the current research, experimental study on abrupt expansion pipe behind plunger valve was carried out, the flow regime and cavitation phenomena were observed through glass tube, and the influence rules of abrupt-expansion on the hydraulic characteristics of valve were analyzed.
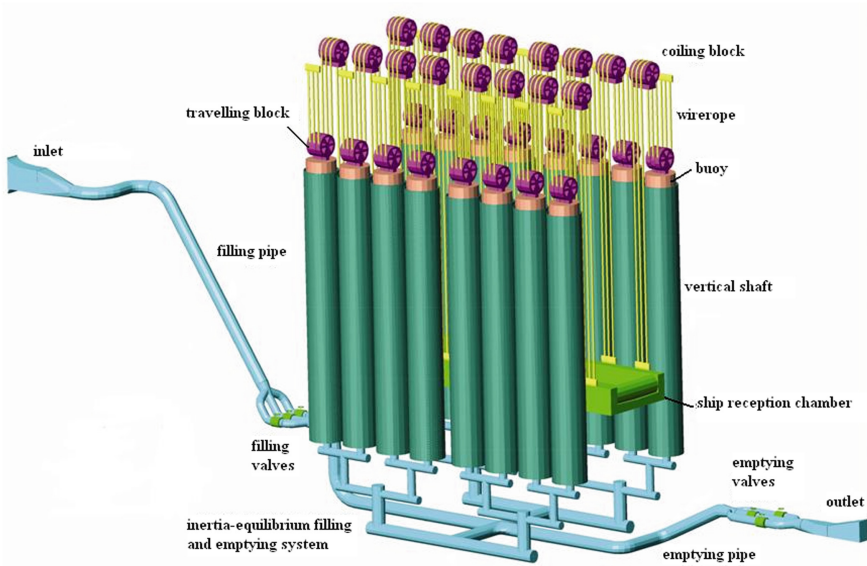
Fig. 1. Jinghong HDSL perspective view.

2 Materials and Methods

In this paper, as seen in Fig. 2, the test valve is a plunger valve, DN = 150 mm, the type of sleeve is SZ20–30% (made by VAG Germany). The experiments were carried out in the multi-functional cavitation experiment hall of Nanjing Hydraulic Research Institute (Nanjing, China). This laboratory is automated with the automatic control of pumps, valves, pressure and flow monitoring. The maximum capacity of water pressure supply system is 1.5MPa and the maximum flow rate is 0.15m³/s. The experimental model is mainly composed by test valve and glass pipe (Fig. 3).

The influence rules of hydraulic characteristics of valve with abrupt-expansion were observed in this study. It mainly includes the properties of flow capacity, wall pressure characteristics and cavitation characteristics. The representative parameters are as follows: flow coefficient (μ), pressure characteristics of pipe after valve including time-average pressure (P_{ta}) and fluctuating pressure (P_{rms}) and cavitation index (K). The main physical quantities required to be observed are as follows: flow rate (Q), cavitation noise, wall pressure, upstream steady pressure (P_u) and downstream steady pressure (P_d). The locations of the sensors are shown in Fig. 4.

In this research, the experimental studies of three kinds of abrupt-expansions were investigated. The specific dimensions of parameters were shown in Table 1, and the definition of expansion ratio (R) was shown in Eq. 1. *ID* and *OD* denote the inside diameter and outside diameter of glass pipe.
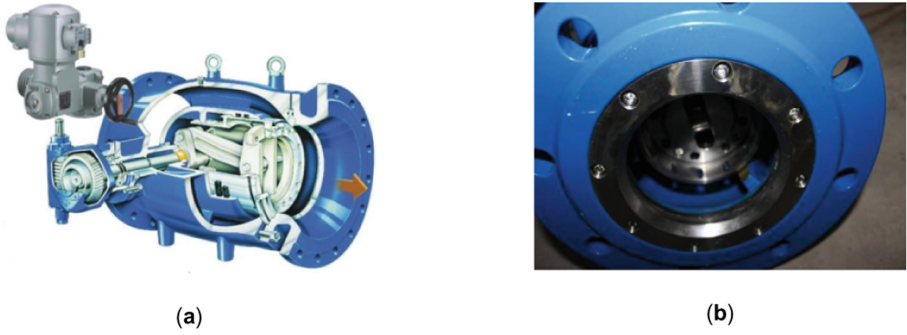
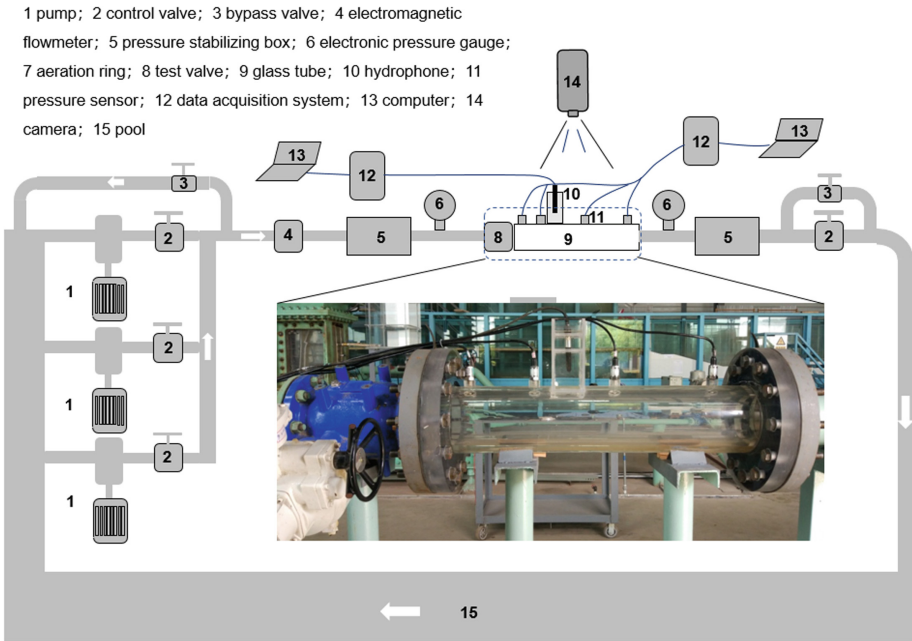**Fig. 2.** (a) Perspective view of plunger valve; (b) Picture of plunger valve.

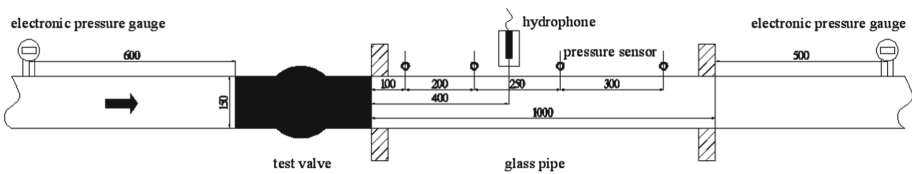1 pump; 2 control valve; 3 bypass valve; 4 electromagnetic
flowmeter; 5 pressure stabilizing box; 6 electronic pressure gauge;
7 aeration ring; 8 test valve; 9 glass tube; 10 hydrophone; 11
pressure sensor; 12 data acquisition system; 13 computer; 14
camera; 15 pool

Fig. 3. Experimental setup.

Fig. 4. Sensor layout (mm).

Table 1. Experiment content.

R	ID (mm)	OD (mm)	L (mm)
1.00	75	105	1000
2.15	110	145	1000
4.00	150	195	1000

$$R = \frac{A_1}{A_2} \tag{1}$$

A_1 denotes the reference section area of abrupt-expansion (m^2); A_2 denotes the reference section area of pipe (m^2).

3   Results and Discussion

3.1   Flow Phenomena

The typical cavitation phenomena of plunger valve are shown in Fig. 5. The cavitation appearances in three types of abrupt-expansions are same. It is mainly misty cavitation. Due to the particular structure of plunger valve, the misty cavitation can be combined into vortex rope cavitation at opening degree of 0.3. Enlarging of the abrupt-expansion size, a thickness of water cushion is added between the cavitation and the pipe wall. For R = 1.00, the pipe is filled with misty cavitation, the collapse of bubbles will directly erode the pipe wall. For R = 2.15, the pipe is basically filled with misty cavitation, but occasionally there is a layer of water cushion between bubbles and pipe wall. For R = 4.00, there is a stable water cushion between cavitation and pipe wall. The process of bubble collapse is confined within the water body, so the impact of collapse on pipe can be buffered, and the pipe vibration and cavitation damage could be reduced significantly.

3.2   Flow Coefficient

In this research, μ is defined as follow:

$$\mu = \frac{Q}{A\sqrt{2\frac{(P_u - P_d)}{\rho}}} = \frac{1}{\sqrt{1 + \sum \zeta}} \tag{2}$$

A denotes the reference section area (m^2); ρ denotes the density of water; g denotes the acceleration of gravity; $\sum \zeta$ denotes the resistance of the test system. Figure 6 and Table 2 show the difference of μ for various R.

From the definition of μ, it can be said that flow loss is the root cause of the change of μ. The resistance of the test system is composed with valve resistance (ζ_v) and abrupt-expansion resistance (ζ_e). The ζ_e includes resistance of the expansion section
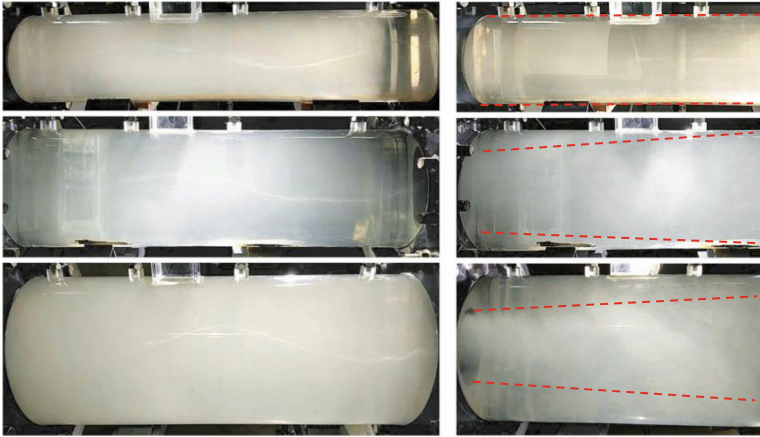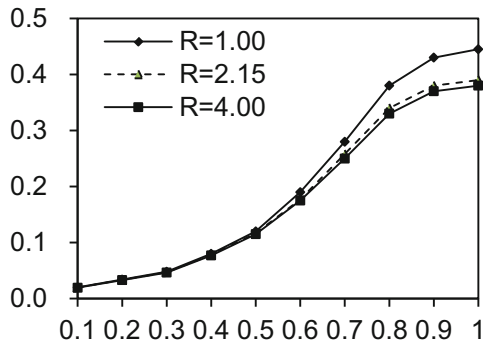
Fig. 5. Cavitation phenomena.

Fig. 6. Flow coefficient for various R.

(ζ_{ex}), resistance along the expansion body (ζ_λ) and resistance of the contraction section (ζ_c), and shown as follows:

$$\sum \zeta = \zeta_v + \zeta_e = \zeta_v + (\zeta_{ex} + \zeta_\lambda + \zeta_c) \tag{3}$$

Because the l/d of abrupt-expansion is large enough (Du et al. 2015), ζ_λ is small and it can be negligible. Therefore, ζ_e can be simplified as:

$$\zeta_e \approx \zeta_{ex} + \zeta_c \tag{4}$$

Section 1 and 2 were defined as shown in Fig. 7. Because the two sections were in the same elevation, so there was no need to consider the potential energy. The relationship of R and ζ_c could be analyzed by theoretical method as follows:

Table 2. Flow coefficient for various R.

n	μ			Decline (%)	
	$R = 1.00$	$R = 2.15$	$R = 4.00$	$R = 2.15$	$R = 4.00$
0.1	0.020	0.0198	0.0195	1.0	2.5
0.2	0.034	0.0335	0.0330	1.5	2.9
0.3	0.048	0.0470	0.0465	2.1	3.1
0.4	0.080	0.0780	0.0770	2.5	3.8
0.5	0.120	0.1165	0.1150	2.9	4.2
0.6	0.190	0.1770	0.1750	6.8	7.9
0.7	0.280	0.2580	0.2500	7.9	10.7
0.8	0.380	0.3400	0.3300	10.5	13.2
0.9	0.430	0.3800	0.3700	11.6	14.0
1	0.445	0.3900	0.3800	12.4	14.6
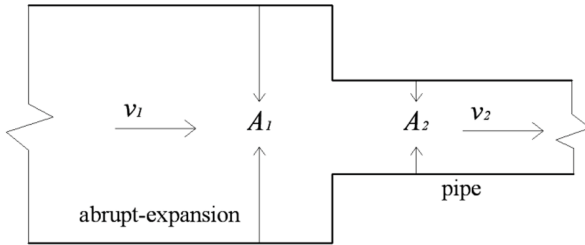
Fig. 7. Abrupt-contraction section.

The Bernoulli's equation considered flow loss:

$$\frac{v_1^2}{2g} + \frac{p_1}{\rho g} = \frac{v_2^2}{2g} + \frac{p_2}{\rho g} + \zeta_c \frac{v_2^2}{2g} \tag{5}$$

The continuity equation:

$$A_1 v_1 = A_2 v_2 \tag{6}$$

The simultaneous solution of Eq. (1)–(6):

$$\mu = \frac{1}{\sqrt{1 + \frac{R^2}{R^2-1} \zeta_c}} \tag{7}$$

In the same way, the influence of R on ζ_{ex} can be analyzed, and combined with Eq. 7:

$$\mu = \frac{1}{\sqrt{1 + \frac{R^2}{R^2-1} \zeta_e}} \tag{8}$$

The empirical formulas of ζ_{ex} and ζ_c are as (Li et al. 2006):

$$\zeta_{ex} = (1 - \frac{1}{R})^2 \tag{9}$$

$$\zeta_c = 0.5(1 - \frac{1}{R}) \tag{10}$$

μ parameter can be obtained as:

$$\mu = \frac{1}{\sqrt{1 + \frac{R^2}{R^2-1}\zeta_e}} = \frac{1}{\sqrt{1 + (1.5 - \frac{2.5}{R+1})}} \tag{11}$$

The impact of R on ζ_e shows in Fig. 8: with the increase of R, ζ_e is increasing, and μ is reducing, but the reducing extent is dropped. For $R = 3$, $\zeta_e \approx 0.9$; for $R = 8$, ζ_e is only 1.2. It can be seen that, when R increases to a certain extent, the further enlargement of R will not have a significant effect on ζ_e. Because the abrupt expansion pipe wall is too far from the mainstream to make a significant impact.
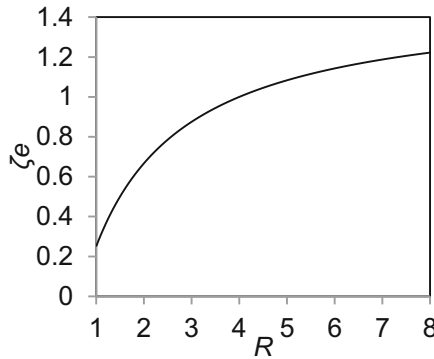

Fig. 8. Relationship of R and ζ_e.

Based on Eq. 11, the formula of μ on the whole test section with R could be obtained:

$$\mu = \frac{1}{\sqrt{1 + \zeta_v + 1.5 - \frac{2.5}{R+1}}} \tag{12}$$

The comparison between theoretical value and measured data of μ is shown in Fig. 9.

It can be seen that the measured data are in good agreement with the theoretical values. Based on the results of above analysis, the variation law of μ can be fully explained.
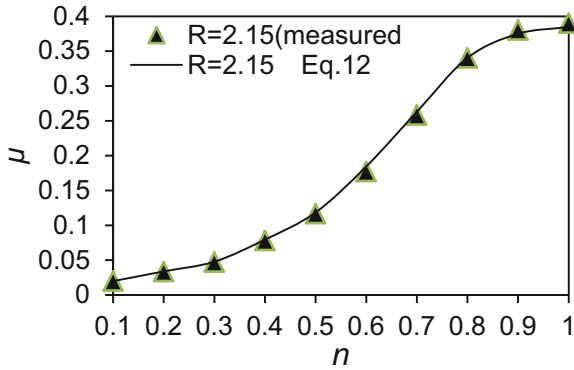
Fig. 9. Comparison of theoretical value and measured data.

For $n = 0.1$–0.5, the variations of μ are very small. Because of ζ_v is much bigger than ζ_e. The influence of abrupt-expansion could be neglected. For $n = 0.6$–1.0, with the increase of n, the ζ_v declined dramatically, and the influence of abrupt-expansion increased remarkably. For R has increased from 2.15 to 4.00, the decrease of μ was 5%, which shown in both of theoretical and experimental results.

3.3   Pressure Characteristics

Figure 10 shows the pressure characteristics for various R values of typical condition. For R increased from 1.00 to 2.15, P_{ta} increased and its maximum promotion was 20 kPa; P_{rms} near valve port decreased significantly and the drop was 2 kPa; For R increased from 2.15 to 4.00, the change of P_{ta} and P_{rms} were very small.
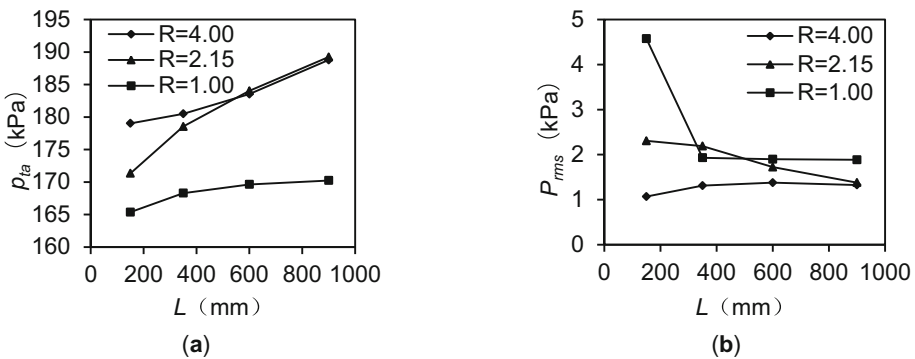

Fig. 10. Pressure characteristics for various R of typical condition. (a) Time-average pressure for various R; (b) Fluctuating pressure for various R.

Combined with pictures of cavitation phenomena, there is a layer of water subfill between pipe wall and mainstream, which is beneficial to increase the P_{ta} after valve, the collapsing of cavitation can be limited within the water body and the P_{rms} can be reduced significantly. After the stable water cushion is formed, the further increase of R, which means the further increase of the thickness of water cushion, has marginal effect on the pressure characteristics of pipe wall.

3.4   Noise Characteristics

As shown in Fig. 11, For R increased from 1.00 to 2.15, time-average sound pressure (SP) dropped rapidly by about 30 Pa, the sound pressure level (SPL) decreased about 40 db in the dominant frequency (6 kHz), and cavitation had been significantly inhibited. For R increased from 2.15 to 4.00, SP and SPL changed slightly. The comparisons of cavitation noise characteristics for various R values in different working conditions are shown in Table 3, it is indicated that when the stable water cushion is formed, the further increase of R wouldn't increase the cavitation suppression effect obviously.
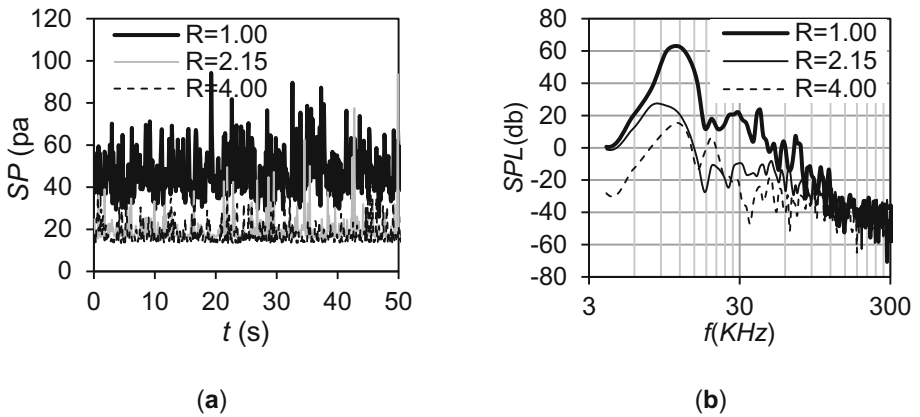

(a)   (b)

Fig. 11. Noise characteristics for various R of typical condition. (a) Sound pressure for various R; (b) Sound pressure level for various R.

Table 3. Cavitation noise characteristics (*CNC*) under different *R*.

Conditions (P_u-P_d, kPa)	CNC	R			Decline (%)	
		1.00	2.15	4.00	1.00 → 2.15	2.15 → 4.00
229-180	SP(Pa)	44.0	15.5	14.0	64.8	9.7
	SP_{rms}(Pa)	10.0	1.0	0.5	90.0	50.0
	SPL(db)	60.0	−15.0	−20.0	125.0	33.3
275-180	SP(Pa)	47.2	20.0	19.0	57.6	5.0
	SP_{rms}(Pa)	11.1	7.6	5.6	31.5	26.3
	SPL(db)	60.0	25.0	20.0	58.3	20.0
325-180	SP(Pa)	205.2	140.5	137.0	31.5	2.5
	SP_{rms}(Pa)	52.5	35.0	24.2	33.3	30.9
	SPL(db)	100.0	70.0	60.0	30.0	14.3

4   Conclusions

(1) Abrupt-expansion reduced the discharge capability of valve. For *n* = 0.1–0.5, the influence was very small. Because of ζ_v was much bigger than ζ_e. The influence of abrupt-expansion could be neglected. For *n* = 0.6–1.0, the influence increased remarkably, because ζ_v decreased with *n* obviously. The variation of μ for various *R* values was smaller for *R* increased from 2.15 to 4.00, because ζ_e decreased slightly with the further increase of *R*.

(2) Abrupt-expansion could improve the pressure characteristics on pipe wall behind valve and inhibit cavitation significantly. There was a layer of water subfill between the wall of abrupt-expansion and mainstream, which could increase the P_{ta}, limit the collapse of cavitation and reduce the P_{rms} significantly.

(3) In order to minimize the influence on the flow coefficient and ensure the formation of stable water cushion, it is suggested that the expansion ratio for this type of abrupt-expansion is suitable for 3.00.

References

Bertoldi D, Dallalba CCS, Barbosa JR (2015) Experimental investigation of two-phase flashing flows of a binary mixture of infinite relative volatility in a Venturi tube. Exp Therm Fluid Sci 64:152–163

Chern MJ, Wang CC (2004) Control of volumetric flow-rate of ball valve using V-port. J Fluids Eng 126:471–481

Du HY (2015) Influence of changed fuel injection pulse width and pressure on discharge coefficient in diesel engine. Trans Chin Soc Agric Eng 31:71–76

Gholami H, Yaghoubi H, Alizadeh M (2015) Numerical analysis of cavitation phenomenon in a vaned ring-type needle valve. J Energy Eng 141:04014053

Han MX, Liu YS, Wu DF et al (2017) A numerical investigation in characteristics of flow force under cavitation state inside the water hydraulic poppet valves. Int J Heat Mass Transf 111:1–16

Hu YA (2011) Basic theory research on hydraulic driven shiplift application. Ph.D. thesis of Nanjing Hydraulic Research Institute, Nanjing, China

Hubballi B, Sondur V (2013) A review on the prediction of cavitation erosion inception in hydraulic control valves. Int J Emerg Technol Adv Eng 3:110–119

Jo SH, Kim HJ, Song KW (2013) A numerical study for reducing cavitation in a butterfly valve with a perforated plate. In: Proceedings of Korean society for fluid machinery, pp 308–308

Kravtsova AY, Markovich DM, Pervunin KS et al (2014) High-speed visualization and PIV measurements of cavitating flows around a semicircular leading-edge flat plate and NACA0015 hydrofoil. Int J Multiph Flow 60:119–134

Lee MG, Lim CS, Han SH (2016) Shape design of the bottom plug used in a 3-way reversing valve to minimize the cavitation effect. Int J Precis Eng Manuf 17(3):401–406. https://doi.org/10.1007/s12541-016-0050-8

Li W (2006) Handbook of hydraulic computation, 2nd edn. China Water Conservancy and Hydropower Press, Beijing

Li WG (2016) Modeling viscous oil cavitating flow in a centrifugal pump. J Fluids Eng 138:011303

Liu YS, Yang YS, Li ZY (2006) Research on the flow and cavitation characteristics of multi-stage throttle in water-hydraulics. Proc IMech Part E: J Process Mech Eng 220:99–108

Long XP, Wang J, Zhang JQ et al (2018) Experimental investigation of the cavitation characteristics of jet pump cavitation reactors with special emphasis on negative flow ratios. Exp Thermal Fluid Sci 96:33–42

Osterman A (2009) Characterization of incipient cavitation in axial valve by hydrophone and visualization. Exp Therm Fluid Sci 33:620–629

Pan SS, Peng XX (2013) Physical mechanism of cavitation. National Defense Industry Press, China

Pennings P, Westerweel J, Terwisga TV (2016) Cavitation tunnel analysis of radiated sound from the resonance of a propeller tip vortex cavity. Int J Multiph Flow 83:1–11

Pham TM, Larrarte F, Fruman DH (1999) Investigation of unsteady sheet cavitation and cloud cavitation mechanisms. J Fluids Eng 121:289–296

Shirazi NT, Azizyan GR, Akbari GH (2012) CFD analysis of the ball valve performance in presence of cavitation. Life Sci J Acta Zhengzhou Univ Overseas Edn 9:1460–1467

Tomov P, Khelladi S, Ravelet F, et al (2015) Experimental study of aerated cavitation in a horizontal venturi nozzle. Exp Therm Fluid Sci 8–18

Wang ZY, Huang BG, Wang Y et al (2015) Experimental and numerical investigation of ventilated cavitating flow with special emphasis on gas leakage behavior and re-entrant jet dynamics. Ocean Eng 108:191–201